Direct Imaging of Shale Gas Leaks Using Passive Thermal Infrared Hyperspectral Imaging

There are many types of natural gas fields including shale formations that are common especially in the St-Lawrence Valley (Canada). Since methane (CH_4), the major component of shale gas, is odorless, colorless and highly flammable, in addition to being a greenhouse gas, methane emanations and/or leaks are important to consider for both safety and environmental reasons. Telops recently launched on the market the Hyper-Cam Methane, a field-deployable thermal infrared hyperspectral camera specially tuned for detecting methane infrared spectral features under ambient conditions and over large distances. In order to illustrate the benefits of this novel research instrument for natural gas imaging, the instrument was brought on a site where shale gas leaks unexpectedly happened during a geological survey near the Enfant-Jesus hospital in Quebec City, Canada, during December 2014. Quantitative methane imaging was carried out based on methane's unique infrared spectral signature. Optical flow analysis was also carried out on the data to estimate the methane mass flow rate. The results show how this novel technique could be used for advanced research on shale gases.

Introduction

Natural gas is an energy resource in great demand worldwide. Regardless of its origin, methane (CH_4) is the major component of natural gas. Shale formations represent an important source of natural gas. There are many types of gas fields including shale formations, which are especially common in the St-Lawrence Valley (Canada) [1]. Dealing with methane diffuse emissions and/or leaks is an important and challenging task from both safety and environmental perspectives. Since methane is colorless, odorless and highly flammable, natural gas leaks can lead to hazardous situations. Methane is also a major greenhouse gas contributing significantly to global warming [2]. Its high global warming potential comes from the fact that methane is a highly infrared-active molecule. For this reason, thermal infrared imaging remote sensing represents one of the best approaches for investigating methane gas clouds, over large areas, and from a safe location.

Passive infrared hyperspectral imaging was indeed previously shown successful for carrying out gas imaging on large distances [3-5]. By fitting the spectral radiance measured at sensor level with a set of unique spectral signatures associated with each gas target, selective chemical imaging can be achieved. However, chemical

Figure 1 Visible image of the shale gas leak site as seen from the sensor location.

imaging of methane gas represents a particular case since it is already omnipresent in the atmosphere at a concentration of 1.8 ppm. Therefore, discriminating atmospheric methane from methane emanating from a leak source requires a more sophisticated approach. As the amplitude of the signal scales with distance, an efficient atmospheric radiative transfer model is required in order to measure leaks over large distances. In addition, there is a strong overlap between the spectral features of atmospheric water vapor and the ones associated with methane, making this task even more challenging. Therefore, in order to successfully

image methane gas clouds (not from the atmosphere) over large distances, high spectral resolution is required to efficiently discriminate methane spectral features from other infrared-active gases. Recent progress in hardware development and signal processing allowed both spectroscopic confirmation and methane quantification, down to ambient level, for all pixels simultaneously, and over distances on the order of hundreds of meters [4-5].

In order to illustrate the potential of passive thermal infrared hyperspectral imaging for research on natural gas, the Telops Hyper-Cam Methane was brought near shale gas leaks that unexpectedly happened during a geological survey near the Enfant-Jesus hospital in Quebec City (Canada) during December 2014 (see Figure 1). Methane was selectively identified in the leak from its unique infrared spectral signature. In this work, preliminary methane quantification results are presented. The results show how this novel technique could be used for imaging natural gas leaks.

Figure 2 Broadband infrared image of the investigated scene.

Experimental Information

Telops Hyper-Cam

The Telops Hyper-Cam is a lightweight and compact hyperspectral imaging instrument that uses Fourier Transform Infrared (FTIR) technology. It features a closed-cycle-stirling-cooled mercury-cadmium-telluride (MCT) focal plane array (FPA) detector, which contains 320×256 pixels over a basic 6.4°×5.1° field of view (FOV). The spectral resolution is user-selectable up to 0.25 cm^{-1} over the entire spectral range of the instrument. The

Hyper-Cam Methane was specifically designed for methane investigation. Its optics and detector are specifically tuned on the methane spectral features, i.e. from 7.4 to 8.2 µm (1230 – 1350 cm^{-1}), in the thermal infrared spectral ranges. A wide-angle demagnifying 0.25× telescope was used for the measurements leading to a FOV of 25.6°×20.4°. The sensor was located at a 50-m distance from the core drilling location, as determined from a laser rangefinder measurement. This lead to an effective imaging pixel size of about 49 cm^2/pixel. The instrument's FOV was narrowed down to 128×256 pixels and the spectral resolution set to 2 cm^{-1} (84 spectral bands). Outside temperature, relative humidity, atmospheric pressure and wind speed during the acquisitions were -11 °C, 50 %, 104.4 kPa and 10-20 km/h respectively.

Radiative Transfer Model

The broadband images associated with the hyperspectral data were obtained by summing, for each pixel, the radiance measured at each wavenumber over the whole FPA detector spectral range. Column density results were estimated by solving Equation 1, where L is the measured radiance at sensor, L_{bkg}, the radiance at the back of the gas plume, ε_{bkg}, the spectral emissivity associated with the background, Dw, the downwelling radiance, τ_{plume} the gas plume transmittance, L_{plume}, the self-emission radiance associated with the gas plume, and L_{atm} and τ_{atm}, the self-emission radiance and transmittance associated with the atmosphere respectively. Self-emission is function of the object's thermodynamic temperature while transmittance is function of gas concentration (expressed in ppm), path length l (expressed in meters) and the gas molar absorptivity κ as expressed in Equation 2.

Equation 1

$$L = \left[(L_{bkg}\varepsilon_{bkg} + (1-\varepsilon_{bkg})Dw)\tau_{plume} + L_{plume}(1-\tau_{plume})\right]\tau_{atm} + L_{atm}(1-\tau_{atm})$$

Equation 2

$$\tau_{plume} = \exp\left(-\sum \kappa l[gas]\right)$$

Results and Discussion

Hyperspectral Imaging

Many materials encountered in outdoor environments behave like infrared grey bodies, i.e. are featureless across all wavelengths. Unlike many common materials, gases like methane (CH_4) and water vapor (H_2O) behave like selective absorbers/emitters of infrared radiation. Their absorption/emission pattern is function of wavelength (or wavenumbers). Therefore, their presence can be easily detected when looking at high spectral resolution infrared data. Hyperspectral imaging allows the recording of such spectra for each pixel. In order to illustrate the great variety of infrared-active material within a scene, the typical spectra associated with selected pixels are shown in Figure 3.

The infrared spectrum associated with a grey body surface should correspond to a straight line (on a brightness temperature scale). However, because of the presence of atmospheric gases in the path located between the infrared sensor and the target, the measured spectrum is highly structured. They are mostly associated with ground-level atmospheric component like water vapor, CH_4, and nitrous oxide (N_2O). Since the atmospheric water content is typically a few orders of magnitude higher than the other components, water spectral features are dominant. The high-resolution infrared spectra associated with a pixel near the drill is quite different and shares many similarities with the methane reference absorption spectrum.

Methane Chemical Imaging

The image contrast obtained using conventional infrared broadband and narrowband imaging is essentially qualitative and cannot be easily translated to any quantitative gas concentration values. As expressed in Equation 1, the amplitude of the signal obtained for each pixel of an infrared remote sensing measurement is function of numerous parameters as expressed in Equation 1 and Equation 2. As opposed to other conventional narrowband infrared gas imaging

technologies, the signal measured by the hyperspectral camera used in this work has some physical meaning as it is expressed in terms of spectral radiance units ($W/sr.m^2.cm^{-1}$). Quantification can then be handled by fitting radiative transfer algorithms (Equation 1) with a non-linear optimization routine [6] in order to estimate the relative contribution of each parameter within the measurement. According to the distance (see Equation 2) estimated with atmospheric components such as water vapor and nitrous oxide (N_2O), the atmospheric methane content can be estimated and then subtracted from the total amount determined in the line-of-sight of each pixel. The "excess" methane contribution was attributed to the shale gas leaks. The results are shown in Figure 4.
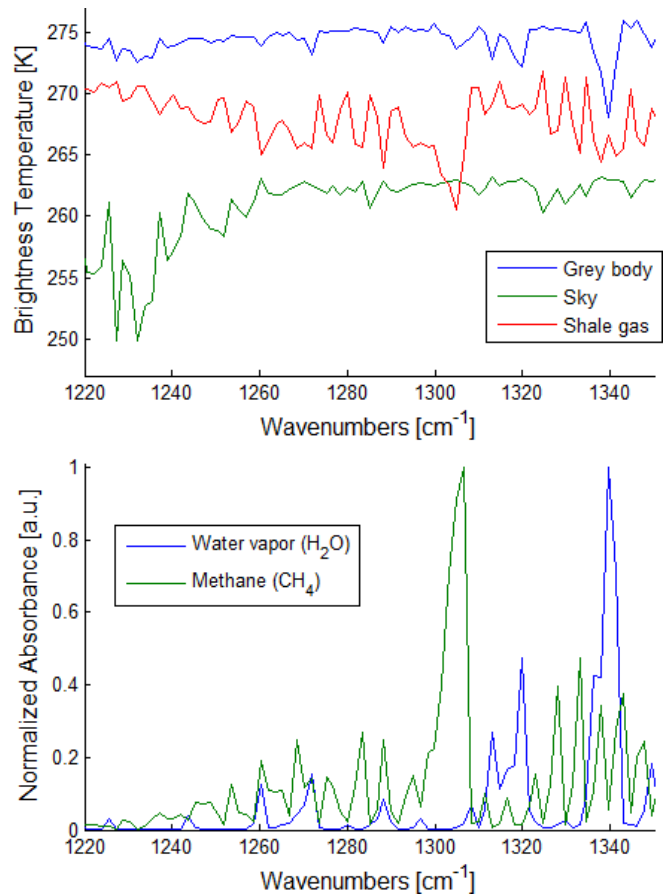

Figure 3   Infrared spectra associated with a single pixel representative of sky radiance, the roof from the rear house, and shale gas (top). The spectra are plotted on a brightness temperature scale for clarity purposes. The reference absorption spectra of water vapor and methane are shown (bottom) for comparison purposes.
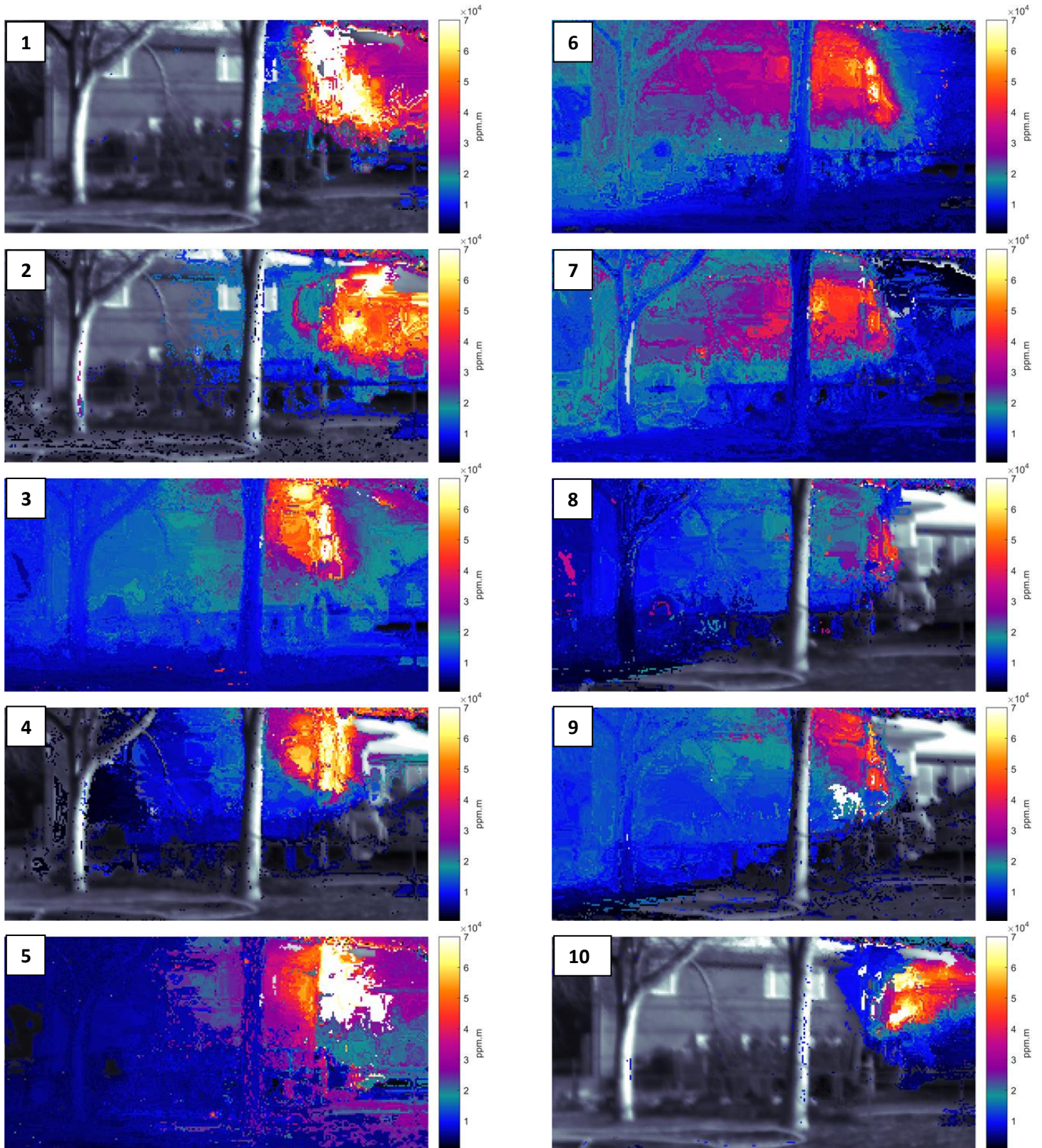
Figure 4 Consecutive methane column density maps (1 to 10) obtained after fitting the radiative transfer model described in Equation 1. Column density estimates are plotted over the broadband infrared image associated with each acquisition for clarity purposes.

As expected, greater gas content (column density) is observed near the drill from where the gas leaks originate. Due to the wind and the high gas pressure of the underneath shale reservoir, methane gas is being spread all over the place, which explains why some positive quantification results can be observed away from the leak source. Sky radiance is usually considered a very good background source. It creates a very high thermal contrast for gas detection since it allows detection at lower concentration values. For this reason, positive methane detections are obtained in the sky area.

The estimated gas column density near the leak source was on the order of 65 000 ppm×m. Assuming a cylindrical symmetry of the gas plume in the center portion, the radius and depth are on the order of 1 m. Therefore, it can be estimated that the methane content in the shale gas is on the order of 6-7 %, which is in good agreement with previous geological surveys carried out on the shale composition of this area [1]. Such leaks represent a very serious situation because such a methane concentration lies within the methane lower/upper explosion limits (LEL-UEL, ~5-15 %). Under these conditions, a deflagration can be initiated by any ignition source such as a spark. The mixture could indeed be ignited be the firefighters on site during the installation of a rescue-flaring unit.

Mass Flow Rates

The Telops Hyper-Cam Methane uses FT-IR technology with which full-frame images are captured for each optical path difference (OPD) mirror position of the Michelson interforemoter at a high velocity. This time-domain data is then converted into a hyperspectral cube, i.e. frequency-domain data, after performing fast Fourier transform (FFT). The high-velocity broadband-like infrared imaging associated with the time-dependant data can be used to estimate the gas cloud velocity using spatio-temporal correlation algorithms [4]. This strategy was found effective for estimating gas mass flow rates in previous works [7]. Using this scheme, the velocities (expressed in m/s) are combined with column density

quantities (expressed in ppm×m) and the dependency over path length (i.e. m) no longer holds. The mean velocity map obtained for a selcted acquisition is presented in Figure 5.
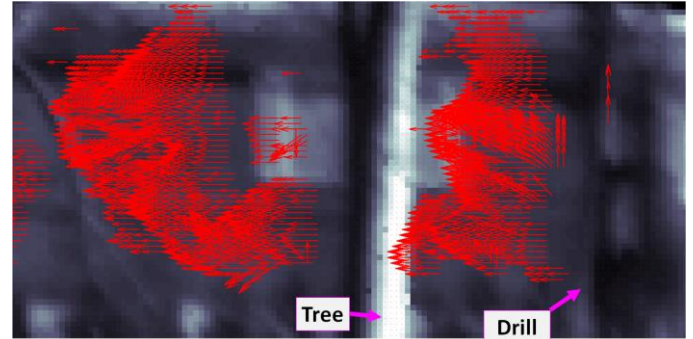

Figure 5 Mean velocity map obtained after optical flow analysis of acquisition #7. The displayed area focuses on the region near the drill for better visualization. The local velocity vectors are represented by red arrows. The velocity estimates are displayed over the broadband infrared image for clarity purposes.

In such a velocity map, the red arrows correspond to local velocity vectors of different orientations and magnitudes. From the median velocity map, it can be seen that the shale gas leak likely originates from the midportion of the drill (as expected). In this particular example, the gas cloud is located behind the front tree, which is why no velocity results can be determined over this area. Weak thermal contrasts were estimated between the gas cloud and the background window belonging to the house. This somehow represents a limitation of the optical flow approach as the spatiotemporal correlation is carried out on the image contrast between the gas plume and its background. For the same reason, this approach does not perform well in weak gas concentration conditions.

The data can then be converted into mass flow rates (expressed in g/s) after the integration over a cross-section of the gas plume. The methane mass flow rate was estimated for each acquisition. The results are presented in Figure 6. It can be seen that the values fluctuate significantly from acquisition to acquisition. The methane gas cloud is significantly driven by cross-wind that keep changing orientation as a function of

time. These fluctuations can also be visualized in Figure 4. Therefore, the mass flow rate estimates associated with the shale gas leaks reported in Figure 6 are convoluted with the local wind speed. Both velocities, i.e. the high-pressure gas leaks and the wind, cannot be easily decorrelated. Still, plotting the values as a function of time provides a good way of getting a rough estimate of the net shale gas leak's mass flow rate.
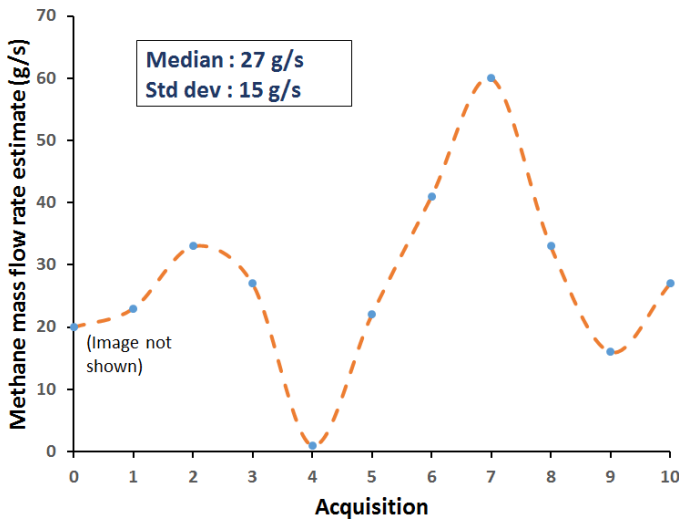

Figure 6 Methane mass flow rate estimates as a function of time.

A median value of 27 g/s of methane was estimated in this case. According to other atmospheric parameters, this should correspond to a methane flow rate of about 2000 L/min.

Conclusion

An accidental shale gas leak resulting from geological activities was successfully visualized using passive thermal infrared hyperspectral imaging. The incident was investigated from a safe location without the need of any additional means such as an illumination source nor any invasive sampling analysis followed by lab analysis. Methane could be selectively identified in the mixture from its unique infrared spectral signature. Here, the methane content was estimated at 6-7 %, which is within the flammable concentration bounds. This emphasizes the need for remote sensing technologies when dealing with natural gas leaks.

References

[1] A. Moritz, J.-F. Hélie, et al., "Methane baseline concentrations and sources in shallow aquifers from the shale gas-prone region of the St. Lawrence lowlands," Environ Sci Technol, 44, pp. 4765-4771, 2015.

[2] D.A. Lashof and D.R. Ahuja, "Relative Contributions of Greenhouse Gas Emissions to Global Warming," Nature, 344, pp. 529-531, 1990.

[3] P. Tremblay, S. Savary, et al., "Standoff gas identification and quantification from turbulent stack plumes with an imaging Fourier-transform spectrometer," Proc. SPIE, 7673, pp. 76730H2-12, 2010.

[4] M. Gålfalk, G. Olofsson, et al., "Making methane visible," Nature Climate Change, 2877, pp. 1-5, 2015.

[5] M. Gålfalk, G. Olofsson and D. Bastviken, "Approaches for hyperspectral remote flux quantification and visualization of GHGs in the environment," Remote Sensing of Environment, 191, pp. 81-94, 2017.

[6] T.F. Coleman and Y. Li, "An Interior Trust Region Approach for Nonlinear Minimization Subject to Bounds," Cornell University, Ithaca, TR93-1342, 1993.

[7] M.-A. Gagnon, J.-P. Gagnon, et al., "Standoff Midwave Infrared Hyperspectral Imaging of Ship Plumes," Proc. SPIE, 9862, pp. 98620H1-9, 2016.

Telops

100-2600 St-Jean Baptiste Ave
Quebec, QC, Canada, G2E 6J5

+1-418-864-7808
sales@telops.com
telops.com